CHEMMEDCHEM

CHEMISTRY ENABLING DRUG DISCOVERY

Accepted Article

Title: The Design of Potent, Selective and Drug-Like RGD αvβ1 Small Molecule Inhibitors Derived from non-RGD α4β1 Antagonists

Authors: Richard Hatley

To be cited as: *ChemMedChem* 10.1002/cmdc.201900359

Link to VoR: http://dx.doi.org/10.1002/cmdc.201900359

A Journal of

ChemPubSoc Europe

WILEY-VCH

www.chemmedchem.org

WILEY-VCH

COMMUNICATION

The Design of Potent, Selective and Drug-Like RGD αvβ1 Small Molecule Inhibitors Derived from *non*-RGD α4β1 Antagonists

Richard J. D. Hatley*[a], Tim N. Barrett[a], Robert J. Slack[a], Morag E. Watson[a], Daniel J. Baillache[a], Anna Gruszka[a], Yoshiaki Washio[a], James E. Rowedder[a], Peter Pogány[a], Sandeep Pal[a], Simon J. F. Macdonald[a]

[a] *Dr. R. J. D. Hatley, Dr. T. N. Barrett, Dr. R. J. Slack, Dr. M. E. Watson, D. J. Baillache, A. Gruszka, Y. Washio, J. E. Rowedder, Dr. P. Pogány, Dr. S. Pal, Dr. S. J. F. Macdonald*
GlaxoSmithKline (GSK), Medicines Research Centre, Gunnels Wood Road, Stevenage, SG1 2NY (UK).
E-mail richard.j.hatley@gsk.com.

Supporting information for this article is given via a link at the end of the document.

Abstract: Up to 45% of deaths in developed nations can be attributed to chronic fibroproliferative diseases, resulting in a requirement for effective therapies. The RGD (Arg-Gly-Asp) integrin αvβ1 has recently been investigated for its role in fibrosis disease and warrants therapeutic targeting. Herein, we describe (i) the identification of *non*-RGD hit small molecule αvβ1 inhibitors; (ii) that αvβ1 activity is embedded in a range of literature α4β1 (VLA-4) ligands; (iii) how, for the first time, a *non*-RGD integrin inhibitor (of α4β1 in this case) was converted into a potent *non*-zwitterionic RGD integrin inhibitor (of αvβ1 in this case); (iv) the design of urea ligands with excellent selectivity over α4β1 and the other αv integrins (αvβ3, αvβ5, αvβ6, αvβ8); (v) how *in silico* docking models and density functional theory (DFT) calculations aided the discovery of the lead urea series.

Fibrosis is characterized by the build-up of collagen rich components of the extra cellular matrix (ECM) and the layering of excessive scar tissue in response to chronic injury. Eventually, this leads to organ dysfunction and failure, as depicted by fibrotic diseases such as idiopathic pulmonary fibrosis (IPF), liver cirrhosis and kidney fibrosis – all with poor patient survival rates. Indeed, it is estimated that nearly 45% of all deaths in the developed world are the result of various fibrotic disorders, which highlights the requirement for further treatments to meet this growing burden.[1] A large number of biological mechanisms have been targeted for the treatment of fibrotic conditions[2] but the αv-integrins (RGD family) remain an attractive proposition because of their role in activation of TGFβ, a key cytokine regulator of fibrosis.[3]

The 24 known integrins, classified into various sub-families, function as αβ-heterodimeric signalling proteins with structures spanning cellular membranes.[4] In addition to fibrotic diseases, they have already been widely targeted for the treatment of cancers, thrombosis and osteoporosis – investigated with synthetic peptides, antibodies and small molecules.[5] Integrins bind endogenous ligands containing short peptidic recognition sequences, as observed in the therapeutically important family, RGD (Arg-Gly-Asp). It consists of αvβ1 and homologous members αvβ3, αvβ5, αvβ6, αvβ8, along with three other RGD integrins (α8β1, αIIbβ3 and α5β1), not discussed here.

While extensive target validation for αv-integrins in fibrosis exists for αvβ6,[6] some attention has recently focussed on αvβ1, after reports of compelling pre-clinical target validation in fibrosis disease with the design and use of the first αvβ1 selective RGD small molecule mimetic **1** (Figure 1). It has been shown that **1** impressively reduced fibrosis in lung, liver and kidney *in vivo* models, leading the authors (Reed *et al*) to state that "compounds based on this lead compound could be broadly useful for treatment of diseases characterized by excessive tissue fibrosis".[7]

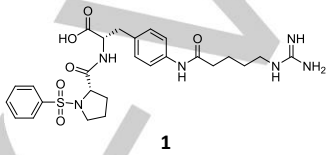

1

Figure 1. Reported αvβ1 selective ligand

However, compound **1** has poor PK properties which makes *in vivo* investigation difficult. In addition, while **1** delivers exquisite αv selectivity, it has recently been shown to have additional β1 activities, which may complicate further TV studies.[8] Historically, identifying low dose, orally bioavailable and selective molecules suitable for clinical use has been highly challenging.[5c,9] Some of the reasons behind this are the polar zwitterionic pharmacophore which usually limits permeability and that many of the integrins have similar binding domains. Approaches have been investigated to improve oral PK properties by attenuating the high polarity in the design of *non*-zwitterionic – *non*-RGD mimetics. However, very few genuine *non*-RGD integrin inhibitors exist, most are either pan-assay interference compounds (PAINS), not easily optimised, or *non*-drug like, thus make unsuitable leads for progression to clinical candidates. [10, 11]

During this work to identify new ligands of the αvβ1 integrin, we describe how we have started to address some of frequently encountered drug design problems, especially the selectivity and the zwitterionic nature. Specifically, we detail; (i) the identification of *non*-RGD hit small molecule αvβ1 inhibitors; (ii) that αvβ1 activity is embedded in a range of literature α4β1 (VLA-4) ligands; (iii) how, for the first time, a *non*-RGD integrin inhibitor (of α4β1 in this case) was converted into a potent *non*-zwitterionic RGD integrin inhibitor (of αvβ1 in this case); (iv) the design of urea ligands with excellent selectivity over α4β1 and the other αv integrins (αvβ3, αvβ5, αvβ6, αvβ8); (v) how *in silico* docking models and density functional theory (DFT) calculations aided the discovery of the lead urea series. With many inhibitors of α4β1 known,[12] we show that this innovative approach, of converting a *non*-RGD ligand to an RGD ligand, could be of particular value in providing a rich source of new chemotypes for inhibiting αvβ1, but may also catalyse the

discovery of new ligands for the other closely related αv-integrins.

There is a paucity of literature αvβ1 SAR data and structural information to guide the rational design of new inhibitors. We therefore took the approach to identify potential hits from the GSK data bank of diverse compounds, already with a pedigree for inhibiting various integrins. Compounds were selected and tested at a fixed concentration (1 μM) in a fluorescence polarization assay against three αv-integrins; αvβ1, αvβ5 and αvβ6, allowing rapid identification of potential inhibitors with simultaneous generation of αv-selectivity data. Assessment of the output revealed unanticipated but striking results where one set of structurally related molecules, containing the biphenyl α-amino acid core template, appeared to robustly show exquisite selectivity for αvβ1 over both αvβ5 and αvβ6, as exemplified by **2** and **3** (Table 1). The high potency and selectivity of the hit compounds was confirmed after wider screening in all five αvβx cell adhesion assays (x=1,3,5,6,8)[13] and in αvβ1/α4β1 radioligand binding assays (See Table 1 and SI for methodology). First indications of integrin cross reactivity came with RGD peptides some time ago but has not seen further exploration.[14]

Table 1. Exemplar αvβ1 hit molecules obtained from α4β1 templates

	Structure	Potency and Selectivity#	Physchem properties
2	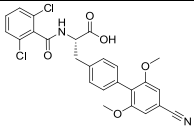	αvβ1 pIC_{50} 5.8 αvβ3, 5, 6, 8 pIC_{50} <5 αvβ1 pKi 7.41 α4β1 pKi 9.85 **(x275 sel. for α4β1)**	MW 499 $ChromLogD_{7.4}$ 2.8 BEI* 11.6 (14.8)
3	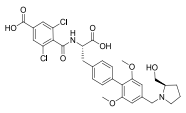	αvβ1 pIC_{50} 7.4 αvβ3, 5, 6, 8 pIC_{50} <5 αvβ1 pKi 9.01 α4β1 pKi 9.71 **(x5 sel. for α4β1)**	MW 632 $ChromLogD_{7.4}$ 0.13 BEI* 11.7 (14.3)

GSK cell adhesion data (pIC_{50}) – mean of at least 2 assay test occasions; radioligand data (pKi) – mean of 2 assay test occasions. *BEI[15] calculated from αvβ1 pIC_{50} and (pKi).

This result was very surprising given that the close homology in αv integrin binding sites normally precludes high selectivity for one αv-isoform.[5c] Moreover, it was unexpected to find that the hit compounds originated from legacy series of α4β1 inhibitor molecules, thus demonstrating unusual cross reactivity across the integrin families (RGD and *non*-RGD) – the α4β1 integrin belongs to the leukocyte integrin family (not RGD) with different ligand recognition sequences to RGD.[16]

Before optimizing the dual active hit molecules (α4β1-αvβ1) to improve potency and selectivity for αvβ1, we explored the generality of this finding and only found one example from the literature – a series of aryl sulfonamide pyrimidines with activity at both αvβ1 (0.5μM) and α4β1 (9nM).[17] However, with no other indication of this dual activity being reported, we screened additional structurally related α4β1 small molecules from the literature at αvβ1 (eg. **4**, Table 2) and found that the connection of embedded dual activity began to strengthen, although the activity at α4β1 was always higher. During this work, we also found that compound **1** also unexpectedly contained high α4β1 activity, pK_d 9.11.[8] These data collectively show that αvβ1 activity is likely to be present in a number of distinct α4β1 chemotypes and should be taken into account for future target validation studies. In light of uncovering this dual activity, optimization of any αvβ1 inhibitors would benefit by having selectivity over α4β1 as well as the other αv integrins.

Table 2. Selected literature molecules demonstrating dual αvβ1-α4β1 activity

	Structure	Potency and Selectivity#	Physchem properties
1[a]	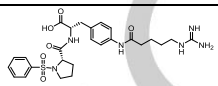 CAS no. 1689540-62-2	αvβ1 pKd 9.57 α4β1 pKd 9.11 **(x2.9 sel. for αvβ1)**	MW 559 $ChromLogD_{7.4}$ 0.68
4[b]	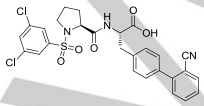 CAS no. 217325-56-9	αvβ1 pKi 8.51 α4β1 pKi 9.70 **(x15.5 sel. for α4β1)**	MW 573 $ChromLogD_{7.4}$ 3.7
5[c]	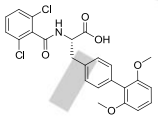 CAS no. 232271-19-1	αvβ1 pKi 6.50 α4β1 pKi 9.13 **(x427 sel. for α4β1)**	MW 474 $ChromLogD_{7.4}$ 2.7

[a] Reported data: αvβ1 IC_{50} 0.089-0.63 nM.[7,18] [b] Reported data: α4β1 IC_{50} 0.46 nM.[19] [c] Reported data: TR-14035 α4β1 IC_{50} 87 nM.[20] #GSK Radioligand data (pKi or pKd) – mean of 2 assay test occasions.

The hit compounds containing the biphenyl α-amino acid backbone showed the expected binding mode to αvβ1 as depicted by the *in silico* docking and served as the basis for future molecule design (See Figure 2 and SI for methodology). Elevated potencies were readily achieved by the incorporation of simple functional groups to the unsubstituted bis-methoxy biphenyl **5**, to give for example, nitrile **2** and prolinol **3**. The general finding was that the hit compounds exhibited good potency at αvβ1 with inherent selectivity over the αv integrin family members, although with concomitant high activity at α4β1, as expected. It is therefore highly notable that in contrast to almost all other small molecule αv-RGD inhibitor structures, hit molecules here lacking the Arg mimetic (see **2**, **3**, **4**, and **5)** can be considered as *non*-RGD inhibitors of the RGD integrin αvβ1. This is presumably driven in part by maximizing other interactions within the β1-subunit, such as the acid-metal interaction in the metal-ion dependent adhesion site (MIDAS), the π-π interaction with Tyr178 and/or with interactions to the benzamide moiety (See Figure 2).

The hit compounds are also considerably less polar than **1** as determined by the higher ChromLogD values[21] and may therefore help to increase permeability. Hit molecule **2** was a reasonable start point for further optimization because of its structural similarity to the oral clinical compound firategrast[5b] – a dosing route advantage over many other αv integrin inhibitors. During the optimization of the hits, the ligand efficiency metric (BEI

efficiency measure)[15] was used to establish which structural changes were most beneficial. At the outset, this revealed that the hit compounds (eg. **2**) generally exhibited low efficiency at αvβ1, mainly because of the moderate potency, but we show how the molecules were efficiently optimized to give better profiles (*vide infra*).

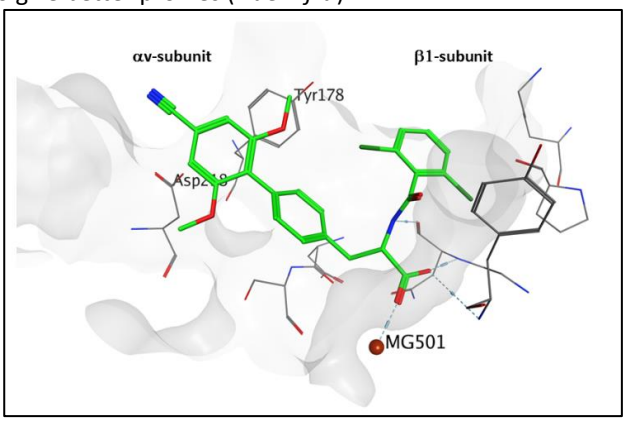

Figure 2. Docking of *non*-RGD hit **(2)** in an αvβ1 homology model showing good π-π stacking of the bismethoxy benzonitrile with Tyr 178 (Note the absence of interactions with Asp218, the normal observed Arg binding amino acid in RGD inhibitors).

The wider αvβ1 SAR around molecule **2** was quickly established by the testing of available close analogues not previously screened, but also through the synthesis of additional analogues, still lacking an Arg binder (data not shown). The first intent was to determine the minimum structural features responsible for good potency (ie. pharmacophore) and high ligand efficiency. However, it was found that most of the functional groups already present in these GD hits were required for binding. This was not a surprise, given the curtailed binding opportunity ie. without the Arg binder. Nevertheless, potential efficiency improvements were envisaged in the β-region by replacing the bulky dichlorobenzamide group or bismethoxy benzene appendages with lower MW alternatives, but this proved to be challenging. A potency advantage came with installation of a para-carboxylic acid, present in **3**, which forms a putative salt-bridge interaction with Lys182, giving a potency increase of 1 log unit (see SI-homology models for docking schematic). Yet, evaluation of this hit series early on indicated that any potency advantages would likely be outweighed by the sub-optimal oral drug-like properties, therefore we took the decision to pursue an alternative lead.

Given that the *non*-RGD hit molecules were not of suitably high αvβ1 potency, we hypothesized that improvements may be achieved by introducing a motif with modulated binding to Asp218, in the αv-subunit akin to the traditional full RGD mimetics. This would also give a potential property advantage, overcoming the requirement for a strongly basic group, such as guanidine, which could otherwise limit permeability – a common design problem encountered in the quest for oral RGD mimetics and hence our keen interest to maintain as much of the oral property space held by these αvβ1 GD type hits. Visual inspection of αvβ1 and α4β1 integrin *in silico* homology models (See SI for methodology) indicated that incorporation of a polar motif to the α4β1 molecules in the αv subunit could potentially reduce binding to α4β1 (due to lack of interaction with lipophilic residues) but concomitantly elevate αvβ1 activity (due to an interaction with Asp218). We reasoned that a *non*-basic binding motif to Asp218 in the form of a urea, which has precedence in αvβ3,[22] might serve to meet the desired potency, selectivity and physicochemical requirements. To test the hypothesis, novel phenyl urea **6** (Table 3) was rapidly synthesized in 3 steps from commercially available materials (See Figure 3 and SI) then tested for activity in cell adhesion and radioligand assays.

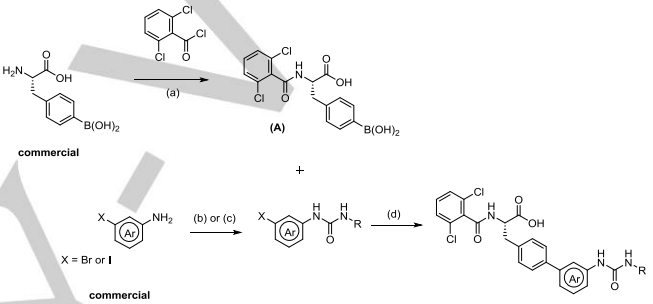

(a) Na_2CO_3, $MeCN/H_2O$ (b) RNCO, $CHCl_3$, 110 °C (c) 4-NO_2PhOCOCl, pyr, CH_2Cl_2 then $ArNH_2$ (d) **(A)**, $Pd(dppf)Cl_2$, K_3PO_4, THF/H_2O, 110 °C.

Figure 3. General synthesis of αvβ1 urea inhibitors

Phenyl urea **6** showed a dramatic selectivity switch now in favour of αvβ1 over α4β1 (x21 fold) and represented the breakthrough lead that delivered on potency and selectivity (See Table 3). It gave the expected docking pose in the αvβ1 homology model, showing a bidentate interaction between the urea and the Asp218 residue located in the α-subunit,

Table 3. Urea hit

	Structure	Potency and Selectivity#	Physchem properties
6	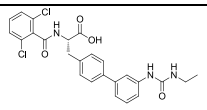	αvβ1 pIC_{50} 5.9 αvβ3, 5, 6, 8 pIC_{50} <5 αvβ1 pKi 8.22 α4β1 pKi 6.89 **(x21 sel. for αvβ1)**	MW 500 $ChromLogD_{7.4}$ 2.1 BEI* 11.8 (16.4)

GSK Radioligand data (pKi) – mean of 2 assay test occasions; cell adhesion data (pIC_{50}) – mean of at least 2 assay test occasions. *based on αvβ1 cell adhesion and (radioligand) data.

which is absent in α4β1 (Figures 4a & 4b) and thus provides an explanation for the observed selectivity switch, favouring αvβ1. While the potency for **6** at αvβ1 was within the range of original hits **2** and **3**, improvements in ligand efficiency were clearly evident (BEI 16.4 vs. 14.8 & 14.3), thus allowing greater scope for incorporation of additional structural modifications that may be of benefit. The absence of the methoxy groups aided an increase in BEI and is thought to provide increased structural flexibility for binding to Asp218 while maintaining the acid-metal interaction. It was pleasing

to observe that activity at other αv integrin members was still absent (pIC_{50} <5).

a

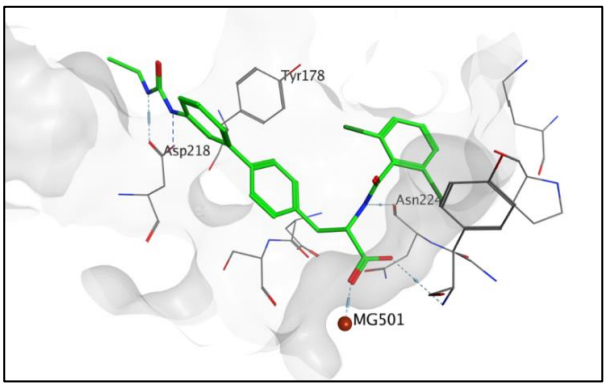

b

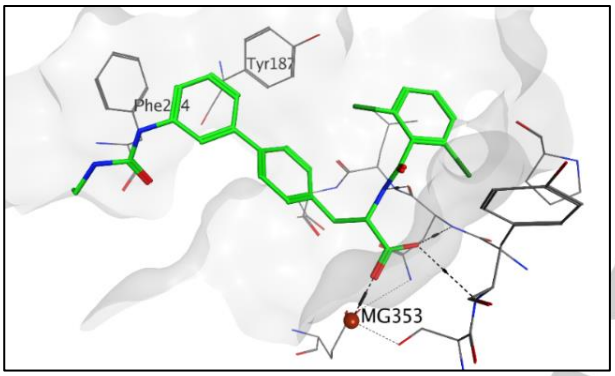

Figure 4. a) Docking of lead urea **(6)** in the αvβ1 homology model showing a robust urea bidentate interaction with Asp218. b) Docking of lead urea **(6)** in the α4β1 homology model, unable to effectively bind the urea motif.

The biaryl urea amide series now offered an αv pharmacological profile clearly differentiated from the reported αvβ3 urea sulfonamide series,[22b] which is devoid of αvβ1 activity (see closely related analogue **7** for comparison, Table 4). With the urea group (in combination with a biaryl amide) now firmly established as essential for binding and selectivity, the structural requirements of the aryl urea motif itself were next probed. It was found that direct attachment (without a spacer) of the urea to the *meta* position (preferred over *para*) on the aromatic ring was optimal (see **8** and SI for additional analogues). In addition, no significant advantages were gained by changing the ethyl group pendant to the urea terminus (see SI for further examples) although this strategy has shown to increase selectivity for αvβ6 in cyclic peptides.[23] Consequently, the biaryl *meta* urea template as contained in **6** was kept unchanged to investigate how increases in potency could be achieved.

We further hypothesized that reducing the electron density of the terminal phenyl ring could serve to increase the urea binding interactions in two ways; (i) by increasing urea NH polarization to effect stronger hydrogen bonding to Asp218 and (ii) by increasing favourable π-π interactions with the electron rich residue Tyr178 (See Figures 2 and 4). DFT calculations (Table 6 and SI for methodology) showed that (i) predominates over (ii) and additionally, from dihedral scanning, the geometry of the urea is affected by the electronics of the attached aryl ring, impacting the binding conformation (*vide infra*).

Table 4. SAR of selected urea molecules

	Structure	Potency and Selectivity^	Physchem properties
7[d]	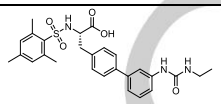	αvβ1 pIC_{50} <5 αvβ3 pIC_{50} 6.2 αvβ5 pIC_{50} 6.1 αvβ6 pIC_{50} <5	MW 510 ChromLogD$_{7.4}$ 3.0 BEI* << 9.8
8	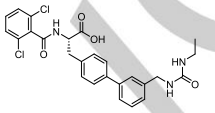	αvβ1 pIC_{50} 5.7 αvβ3,5,6,8 pIC_{50} <5	MW 514 ChromLogD$_{7.4}$ 2.2 BEI* 11.1
9	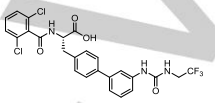	αvβ1 pIC_{50} 6.4 αvβ3,5,6,8 pIC_{50} <5	MW 502 ChromLogD$_{7.4}$ 2.7 BEI* 15.7

[d] close analogue to that already reported[22b] ^GSK cell adhesion data (pIC_{50}) – mean of at least 2 assay test occasions. *based on αvβ1 cell adhesion data.

To test this hypothesis, the electronic properties were initially probed by substituting fluorine atoms at each of the four sites on the benzene ring (adjacent to the urea as in **10**, Table 5) – synthesized according to Figure 3. Increases in potency at αvβ1 were immediately obtained for three of the four F analogues (αvβ1 pIC_{50} 6.4-6.8) vs. pIC_{50} 5.9 for the unsubstituted urea **6**.

Table 5. Advanced αvβ1 leads

	Structure	Potency and Selectivity#	Physchem properties
10	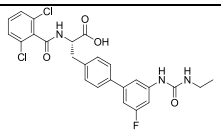	αvβ1 pIC_{50} 6.8 αvβ3, 5, 6, 8 pIC_{50} <5 αvβ1 pKi 8.89 α4β1 pKi 6.71 **(x151 sel. for αvβ1)**	MW 518 ChromLogD 2.5 BEI* 13.1 (17.1)
11	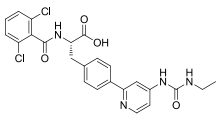	αvβ1 7.8 αvβ6 5.3 αvβ8 6.1 αvβ3, 5 pIC_{50} <5 αvβ1 pKi 9.94 α4β1 pKi 7.52 **(x263 sel. for αvβ1)**	MW 501 ChromLogD 1.6 BEI* 15.6 (19.8)
12	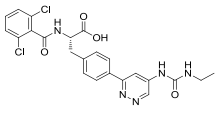	αvβ1 pIC_{50} 7.9 αvβ3, 5, 6 pIC_{50} <5 αvβ8 pIC_{50} 6.2 αvβ1 pKi 9.78 α4β1 pKi 7.11 **(x468 sel. for αvβ1)**	MW 502 ChromLogD 1.2 BEI* 15.7 (19.5)

GSK Radioligand data (pKi) – mean of 2 assay test occasions; cell adhesion data (pIC_{50}) – mean of at least 2 assay test occasions. *based on αvβ1 cell adhesion and (radioligand) data.

The *meta*-F analogue **10** conferred the highest potency (pIC_{50} 6.8, pKi 8.9) for only a slight increase in MW compared

to hit **6** (F for H), translating to a higher BEI (17.1 vs. 16.4). Importantly, the trend for increased selectivity over α4β1 continued, mainly by increasing potency at αvβ1 – compare fluoro phenyl urea analogue **10** (αvβ1:α4β1 sel. x151) with the unsubstituted phenyl urea **6** (αvβ1:α4β1 sel. x21). Further empirical support that the hydrogen bond donating ability of the urea is crucial for binding to Asp218 was observed with the electron deficient trifluoromethyl urea **9** (Table 4), which gave an increase in potency of 0.5 log compared with hit urea **6**.

In order to raise the αvβ1 potency and selectivity still further, with the hypothesis on urea hydrogen bonding strength appearing to be valid, it was envisaged that electron deficient aromatic groups such as pyridines could serve to further enhance binding interactions. This was supported by DFT calculations (See Table 6 and SI for methodology).

Table 6. Calculated complexation energies of the aryl urea with Asp218 and Tyr178

	Ligand-Asp218 (kcal/mol)	Ligand-Tyr178 (kcal/mol)
6	-19.31	-8.26
10	-22.84	-4.77
11 protonated	-32.13	-5.89
(deprotonated)	(-23.81)	(-4.79)
12	-25.49	-5.31

The trend in the ligand-Asp218 complexation energy was similar to the measured activity, whereas no trend was observed with the ligand-Tyr218 complexation energy, although clearly this interaction contributes to the potency. Each pyridine isomer was synthesized in the same way as previous molecules (Figure 3) and immediately, elevated potencies were obtained, compared with the fluorobenzene matched pairs – in all but one isomer (pyridyl isomers: αvβ1 pIC_{50} 5.5-7.8 vs. fluorobenzene isomers: αvβ1 pIC_{50} 6.4-6.8, see Table 5 and SI). Pyridine **11** delivered the highest potency at αvβ1 (pIC_{50} 7.8, pKi 9.94) – an increment of >1.5 log units from lead urea **6** (pKi 8.22). The selectivity over α4β1 continued to widen (x263 fold). Interestingly, pyridyl isomer **11** was considerably more basic than the other pyridyl isomers (measured pKa 6.3 vs. 3.4-4.9), with the protonated form expected to give a substantial reduction in electron density and deliver stronger interactions with the receptor by ~8.5 kcal/mol. It is interesting to note that the functional groups leading to increased αvβ1 binding also introduced weak activity at αvβ6 and αvβ8, reinforcing the point that subtle changes in the electron density and structure of the ligand in the αv-subunit binding site may impact on potency and selectivity across all the αvβx family members. Alternative heteroaromatic groups, as in the case of the *non*-basic pyridazine heterocycle **12** (measured pKa 4.0) also delivered high potency, presumably the result of the large dipole moment[24] compared to **6**, enabling stronger interactions with Asp218. Thus far, pyridazine **12** delivered the best combination of potency and selectivity for αvβ1 over α4β1, approaching an impressive 500-fold window. For optimized leads **11** and **12**, the BEI was significantly improved over hit urea **6**, by >x1000 fold, allaying initial concerns over the low efficiency start points.

The potency of pyridine **11** is very similar to that of pyridazine **12**, explained by the stabilisation energy of the ligand-Asp218 interaction for **12** falling between the energies of protonated and deprotonated pyridine forms of **11**. In addition, the lowest energy state urea conformations could also be a minor factor to help explain potency differences between urea **6** and the less electron rich systems of **10**, **11** and **12**. (See SI for dihedral energy plots). The *trans* urea conformation was calculated to be more stable in phenyl urea **6** (+0.28 kcal/mol for *cis*) thus causing an energy penalty for delivering bidentate binding to Asp218. In the case of compound **10**, the energy difference between *cis* and *trans* was negligible (+0.03 kcal/mol), but for potent ureas **11** and **12**, the *cis* conformation was highly favoured (+0.52 & +1.48 kcal/mol for *trans*), allowing effective bidentate interaction with Asp218.

It is anticipated that the developability of the urea series *in vivo* could take a similar path to the structurally related templates of historic α4β1 molecules, where high oral bioavailability required an ester prodrug.[25] Preliminary work however, showed that several urea parent compounds had good passive permeability, such as **10** (MDCKII-MDR1 Pexact 77 nm/s). Compound **10** also demonstrated low *in vitro* clearance in rat and human liver S9 fractions (<0.6 ml/min/g tissue) which suggests a reasonable level of metabolic stability – (see SI for assay details). The wider selectivity profile for compound **10** against numerous targets was also very good (See SI for full list).

In conclusion, this work describes for the first time, the identification of *non*-RGD dual α4β1-αvβ1 ligands and their subsequent conversion into highly potent and selective RGD αvβ1 inhibitors, by the incorporation of a *non*-basic aryl urea as the Arg mimetic. This lead urea series has developability advantages, such as ease of synthesis and high selectivity over α4β1, compared to previously described molecules. Additionally, this *non*-zwitterionic and *non*-peptidic template could serve benefit for the design of good oral properties – this remains the subject of future optimization.

Acknowledgements

The authors wish to acknowledge the helpful comments made by the reviewers.

Conflict of interest

The authors declare no conflict of interest.

Keywords: αvβ1 integrin • RGD integrin inhibitors • drug design • α4β1 integrin • medicinal chemistry

[1] a) T. A. Wynn, *J. Pathol*. **2008**, *214*, 199–210; b) S. L. Friedman, D. Sheppard, J. S. Duffield, S. Violette, *Sci Transl. Med*. **2013**, 5, 167sr1.
[2] C. B. Nanthakumar, R. J. D. Hatley, S. Lemma, J. Gauldie, R. P. Marshall, S. J. F. Macdonald, *Nat. Rev. Drug Discov*. **2015**, *14*, 693-720.
[3] N. C Henderson, D. Sheppard, *Biochim. Biophys. Acta*. **2013**, *1832*, 891–896.
[4] J. Takagi, B. M. Petre, T. Walz, T. A. Springer, *Cell* **2002**, *110*, 599–611.
[5] a) S. L. Goodman and M. Picard, *Trends in Pharm. Sci.* **2012**, *33*, 405–412; b) D. Cox, M. Brennan, N. Moran, *Nat. Rev. Drug Discov.* **2010***, 9*, 804–820; c) R. J. D. Hatley, S. J. F. Macdonald, R. J. Slack, J. Le, S. B. Ludbrook, P. T. Lukey, *Angew. Chem. Int. Ed*. **2018**, *57*, 3298–332.
[6] a) G. S. Horan et al. *Am. J. Respir. Crit. Care Med*. **2008**, *177*, 56–65; b) Y. Popov et al. *J. of Hepatology* **2008**, *48*, 453–464; c) B. Wang, B. M. Dolinski, N. Kikuchi, D. R. Leone, M. G. Peters, P. H. Weinreb, S. M. Violette, D. Montgomery Bissell, *Hepatology* **2007**, *46*, 1404–1412.
[7] a) N. I. Reed, H. Jo, C. Chen, K. Tsujino, T. D. Arnold, W. F. DeGrado, D. Sheppard, *Sci. Transl. Med*. **2015**, *7*, 288ra79; b) Y. Chang, W.L. Lau, H. Jo, K. Tsujino, L. Gewin, N.I. Reed, A. Atakilit, A.C.F. Nunes, W.F. DeGrado, D. Sheppard, *J. Am. Soc. Neph*. **2017**, *28*, 1998–2005.
[8] A. L. Wilkinson, J. W. Barrett, R. J. Slack, *Eur. J. Pharmacol.* **2019**, *842*, 239–247.
[9] M. E. Duggan, J. H Hutchinson, *Expert Opinion on Therapeutic Patents*, **2000**, *10*, 1367–1383.
[10] L. M. Miller, J. M. Pritchard, S. J. F. Macdonald, C. Jamieson, A. J. B. Watson, *J. Med. Chem*. **2017**, *60*, 3241–3251
[11] J. B. Baell, G. A. Holloway, *J. Med. Chem*. **2010**, *53*, 2719–2740.
[12] G. X. Yang and W.K. Hagmann, *Medicinal Research Reviews*, **2003**, *23*, 369–392.
[13] a) S. T. Barry, S. B. Ludbrook, E. Murrison, C. M. T. Horgan, *Biochem. Biophys. Res. Commun*. **2000**, *267*, 764–769; b) S. B. Ludbrook, S. T. Barry, C. J. Delves, C. M. T. Horgan, *Biochem. J*. **2003**, *369*, 311–318; c) S. J. F. Macdonald et al. *ACS Med. Chem. Lett*. **2014**, *5* 1207-1212.
[14] a) D. M. Nowlin, F. Gorcsan, M. Moscinski, S-L. Chiang, T. J. Lobl, P. M. Cardarelli, *J. Biol. Chem,* **1993**, *268*, 20352–20359; b) P. M. Cardarelli, R. R. Cobb, D. M. Nowlin, W. Scholz, F. Gorcsan, M. Moscinski, M. Yasuhara, S-L. Chiang, T. J. Lobl, *J. Biol. Chem,* **1994**, *269*, 18668–18673; c) P. Sánchez-Aparicio, C. Dominguez-Jiménez, A. Garcia-Pardo, *J. Cell Biol*. **1994**, *126*, 271–279.
[15] C. Abad-Zapatero, J. T. Metz, *Drug Discov. Today* **2005**, *10*, 464–469.
[16] J. S. Desgrosellier and D. A. Cheresh, *Nat. Rev. Cancer* **2010**, *10*, 9–22.
[17] Y-z. Xu et al. *Bioorg. Med. Chem. Lett*. **2013**, *23*, 3070–3074.
[18] N. I. Reed, Y-Z. Tang, J. McIntosh, Y. Wu, K. S. Molnar, A. Civitavecchia, D. Sheppard, W. F. DeGrado, H. Jo. *ACS Med. Chem. Lett*. **2016**, *7*, 902–907.
[19] W. K. Hagmann et al. *Bioorg. Med. Chem. Lett*. **2001**, *11*, 2709–2713.
[20] I. Sircar et al. *Bioorg. Med. Chem*. **2002**, *10*, 2051–2066.
[21] R. J. Young, D. V. S. Green, C. N. Luscombe, A. P. Hill, *Drug Discov. Today* 2011, *16*, 822−830.
[22] a) K. Urbahns, M. Härter, M. Albers, D. Schmidt, B. Stelte-Ludwig, U. Brüggemeier, A. Vaupel, C. Gerdes, *Bioorg. Med. Chem. Lett*. **2002**, *12*, 205–208; b) K. Urbahns, M. Härter, A. Vaupel, M. Albers, D. Schmidt, U. Brüggemeier, B. Stelte-Ludwig, C. Gerdes, H. Tsujishita, *Bioorg. Med. Chem. Lett*. **2003**, *13*, 1071–1074; c) S. Nagashima, S. Akamatsu, E. Kawaminami, S. Kawazoe, T. Ogami, Y. Matsumoto, M. Okada, K-I. Suzuki, S-I. Tsukamoto, *Chem. Pharm. Bull*. **2001**, *49*, 1420–1432.
[23] T. G. Kapp, Maximilian Fottner, O. V. Maltsev, H. Kessler, *Angew. Chem. Int. Ed*. **2016**, *55*, 1540–1543.
[24] N. A. Meanwell, *J. Med. Chem.* **2018**, *61*, 5822–5880.
[25] H. Chanteux, L. Staelens, V. Mancel, B. Gerin, D. Boucaut, C. Prakash, J-M. Nicolas, *Drug Metab. Dispos*. **2015**, *43*, 1381–1391.

10.1002/cmdc.201900359

WILEY-VCH

COMMUNICATION

*Author(s), Corresponding Author(s)**

Page No. – Page No.

Title

Novel αvβ1 inhibitors: The discovery and subsequent optimization of *non*-RGD dual αvβ1−α4β1 ligands resulted in the identification of novel, highly potent and selective aryl urea inhibitors of the RGD integrin, αvβ1.